Solar-Terrestrial Physics, 2017. Vol. 3. Iss. 4, pp. 74–82, DOI: 10.12737/stp-34201708. © INFRA-M Academic Publishing House
Original Russian version A.V. Ishin, N.P. Perevalova, S.V. Voeykov, V.V. Khakhinov
published in Solnechno-Zemnaya Fizika, 2017, vol. 3, iss. 4, pp. 82–92, DOI 10.12737/szf-34201708

FIRST RESULTS OF REGISTERING IONOSPHERIC DISTURBANCES OBTAINED WITH SibNet NETWORK OF GNSS RECEIVERS IN ACTIVE SPACE EXPERIMENTS

A.B. Ishin
Institute of Solar-Terrestrial Physics SB RAS, Irkutsk, Russia, ishin@iszf.irk.ru

S.V. Voeykov
Institute of Solar-Terrestrial Physics SB RAS, Irkutsk, Russia, serg3108@iszf.irk.ru

N.P. Perevalova
Institute of Solar-Terrestrial Physics SB RAS, Irkutsk, Russia, pereval@iszf.irk.ru

V.V. Khakhinov
Institute of Solar-Terrestrial Physics SB RAS, Irkutsk, Russia, khakhin@iszf.irk.ru

Abstract. Global and regional networks of GNSS receivers have been successfully used for geophysical research for many years; the number of continuous GNSS stations in the world is steadily growing. The article presents the first results of the use of a new regional network of GNSS stations (SibNet) in active space experiments. The Institute of Solar-Terrestrial Physics of Siberian Branch of Russian Academy of Sciences (ISTP SB RAS) has established this network in the South Baikal region. We describe in detail SibNet, characteristics of receivers in use, parameters of antennas and methods of their installation. We also present the general structure of observation site and the plot of coverage of the receiver operating zone at 50–55° latitudes by radio paths. It is shown that the selected location of receivers allows us to detect ionospheric irregularities of various scales. The purpose of the active space experiments was to reveal and record parameters of the ionospheric irregularities caused by effects from jet streams of Progress cargo spacecraft. The mapping technique enabled us to identify weak, vertically localized ionospheric irregularities and associate them with the Progress spacecraft engine impact. Thus, it has been shown that SibNet deployed in the Southern Baikal region is an effective instrument for monitoring ionospheric conditions.

Keywords: ionosphere, GNSS, SibNet, Progress.

INTRODUCTION

For ionospheric research, ground-based receivers of Global Navigation Satellite Systems (GNSS) such as GLONASS and GPS are being widely used. Each receiver simultaneously tracks more than two dozen GNSS satellites, using a minimum of two independent frequencies. This allows us to calculate total electron content (TEC) variations in the ionosphere. Thus, the deployment of a network comprising several dozen receivers in a region provides the possibility of simultaneous sounding of the ionosphere with hundreds of satellite–receiver rays. This advantage, the relatively low price, and simplicity of network deployment make it appropriate to apply GNSS to geophysical studies.

Some dense GNSS networks, for example the GEONET network in Japan, have been widely used for many years as a spaced instrument for monitoring ionospheric conditions. Data from these networks are used to study the ionospheric response to solar flares and eclipses [Afraimovich, 2000; Liu, Lin, 2004; Afraimovich et al., 2007], geomagnetic storms [Perevalova et al., 2008; Shimeis et al., 2015], and strong human impacts [Ding et al., 2014; Zherebtsov, Perevalova, 2016]. In recent years, much attention has been paid to the analysis of GNSS signal scintillations [Prikryl et al., 2010; Jiao et al., 2013; Spogli et al., 2013], which provides information on parameters of small-scale ionospheric irregularities causing radio signal to scatter and the quality of radio communication to reduce. Results of all these studies, on the one hand, help to understand more thoroughly the physics of observed phenomena and, on the other hand, enable us to improve GNSS performance: to increase the accuracy of determination of coordinates, to reduce the probability of slips, etc. [Prikryl et al., 2010; Demyanov, Yasyukevich, 2011; Demyanov et al., 2012; Lejeune et al., 2012; Jiao et al., 2013]. For earthquake-prone regions (in particular, for the Baikal rift system), an important applied problem is also to search for responses and possible precursors of earthquakes [Seismoionospheric ..., 2012]. In addition, the array of all GNSS networks can act as a global instrument for exploring near-Earth space [Afraimovich et al., 2013]. However, the distribution of GNSS receivers over the globe is very uneven. The density of GNSS networks in Russia is very low. Until recently, only two GNSS stations worked stably in the large territory of the Baikal region: BADG and IRKT. In 2012, ISTP SB RAS began to deploy a network of permanently operating dual-frequency GNSS receivers.

Due to unique natural features (Lake Baikal, system of rift faults, elevation above sea level, many sunny days per year, etc.), the Baikal region is of great interest for a comprehensive study. This predetermined the development of an advanced array of heliogeophysical instruments in the region, designed for regular observations of the Sun, space weather, geomagnetic field, and ionosphere [Seismoionospheric ..., 2012; Institute ..., 2015]. The GNSS receiver network supplemented the ISTP SB RAS array of instruments.

In 2009–2014, this array [Institute ..., 2015; Seismoionospheric ..., 2012] (near Lake Baikal) was used for a

series of active space experiments (SE) Radar-Progress on recording of ionospheric effects caused by ignition of approach-correction engines (ACE) of the Progress cargo spacecraft (CS) after undocking from the International Space Station (ISS). After consultation with ISTP SB RAS, the CS engine was started when the spacecraft flied over observatories of the Institute [Khakhinov et al., 2011, 2012; Borisov et al., 2012; Khakhinov et al., 2010, 2012, 2013]. It was oriented so that its jet stream was directed toward ground-based instruments. The purpose of the experiment was to detect and simultaneously record jet-induced effects with various geophysical instruments [Lebedev et al., 2014; Eselevich et al., 2016; Lipko et al., 2016; Klunko et al., 2016; Beletsky et al., 2016; Shpynev et al., 2017]. Along with other instruments, a new regional network of GNSS stations (SibNet), developed in ISTP SB RAS, was used to record effects of operation of CS engines. This article describes this network and presents the first results of its use for detecting the ionospheric response to the operation of Progress cargo spacecraft engines.

SibNet. DESCRIPTION OF THE RECEIVING ARRAY

To carry out complex continuous geophysical monitoring of the ionosphere and to determine dynamic parameters of ionospheric plasma irregularities in the Southern Baikal region, a network of constantly operating observation stations with GNSS signal receivers has been deployed (SibNet, Figure 1).

GNSS receivers have been installed in ISTP SB RAS observatories to ensure safety of equipment and continuous operation of SibNet. On the one hand, the relative positioning of receiving stations was chosen in such a way as to cover the largest possible region.

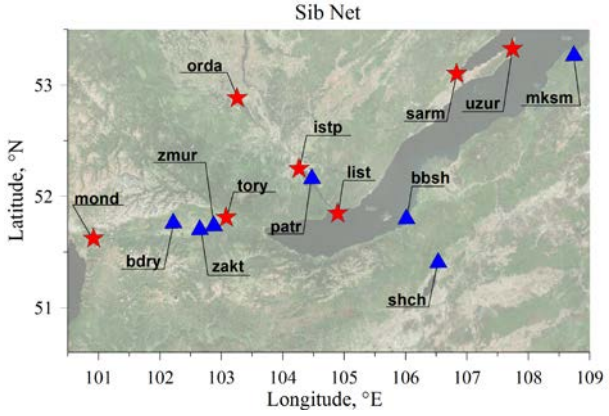

Figure 1. Network of observation stations with GNSS receivers in the Southern Baikal region. Asterisks mark fixed stations; triangles, temporary stations

On the other hand, the velocity and direction of traveling ionospheric disturbances (TID) are calculated using a GPS-interferometry method [Afraimovich, Perevalova, 2006]. For this method to work well, GNSS stations recoding TEC variations should be located at vertices of triangles. In this case, the distance between receivers should not exceed half-wavelength of TID under study. The distance between GNSS stations determines the scale of TIDs whose velocities can be estimated using this network. Examples of measuring triangles with different distances between stations are given in Table 1. Each SibNet station has a GNSS receiver, a control computer, an uninterruptible power supply, and a data transmission channel (Figure 2).

Table 1

Some measuring triangles formed by SibNet stations

Measuring triangle	Distance between stations, km	Scale of TIDs under study, km
MOND–ORDA–LIST	212–160–275	over 600
ORDA–LIST–SARM	160–192–241	over 500
ORDA–ISTP–TORY	98–95–120	over 250
LIST–TORY–ISTP	125–95–62	over 250

SibNet stations are equipped with Delta-G3T and SigmaQ-G3D receivers of Javad GNSS (www.javad.com) [GREIS, 2010]. The Javad GNSS equipment is certified in Russia and listed in a register of measuring equipment (www.ugt.ur.ru).

GNSS radio signals are received with RingAnt-G3T antennas (http://www.javad.com/jgnss/products/antennas) of choke ring type. These antennas have high accuracy, built-in protection against multipath propagation of satellite signal, high stability of phase center position, and also provide a minimum frequency distortion.

In order to enable the use of SibNet data for geodynamic studies, antennas of fixed stations are mounted on specially equipped concrete bases. To minimize the effect of seasonal temperature variations and other local distorting factors, the base is mounted on solid rocks if their bedrock exposures are on the territory of an observatory. An example is the station UZUR of the ISTP SB RAS Baikal Magnetotelluric Observatory (Figure 3). If an observatory is on sedimentary/mantle rocks, the reinforced concrete anchor of the base is placed below the depth of frost penetration. An example is the base built up at the station TORY of the ISTP SB RAS Geophysical Observatory (Figure 4, *a*, *b*). The anchor depth for this base is 4.5 m. In some cases, a receiver antenna is mounted on a wall of an established permanent structure with a rigid anchorage to the main wall. An example of such a station is the station of the ISTP SB RAS Observatory of Radiophysical Diagnostics of the Atmosphere (ORDA) Figure 4, *c*). Parameters of all permanent SibNet stations are shown in Table 2. The Table also presents characteristics of temporary stations deployed during active space experiments.

All antennas are adjusted to the horizontal with the aid of a special device – tribrach (Figure 3, *a*, *b*) – manufactured at ISTP SB RAS. Due to the careful installation of antennas, SibNet data can be used not only to diagnose the behavior of ionospheric plasma, but also to observe the mobility of lithospheric blocks. This greatly increases capabilities of the network.

The Javad Delta-G3T and Javad SigmaQ-G3D receivers can simultaneously receive signals of all visible satellites of GLONASS, GPS, Galileo, and SBAS systems from 216 channels. The receivers perform code, phase, and amplitude measurements for the above satellite systems. The receivers have RS-232 and USB interfaces. In SigmaQ-G3D (station TORY), a multi-antenna (three antennas) GNSS signal reception is accomplished. This allows us to study the small-scale structure

of the ionosphere with spacing of radio paths over a short (about several tens of meters) distance, but at the same time synchronously receive satellite signals. The three-antenna receiver SigmaQ-G3D can be considered as a measuring triangle with an ultra-short distance (about 20–30 m) between the antennas.

The modified models of the Delta-G3T and SigmaQ-G3D receivers, which are used in ISTP SB RAS, make it possible to measure the amplitude of a signal with a frequency of up to 50 Hz to study amplitude scintillations (amplitude measurements). By the scintillations are meant amplitude fluctuations experienced by radio signals propagating through the ionosphere. Ionospheric scintillations indicate signal scattering by electron density irregularities in the ionosphere and lead to a decrease in the signal-to-noise ratio causing slips and a decrease in positioning accuracy. Recording of amplitude scintillations allows us to conduct local observations of small-scale ionospheric disturbances and to assess the navigation-time positioning accuracy.

An important advantage of the Javad GNSS receivers is the open protocol for receiver-to-computer data exchange. Receiver commands and format of internal files (binary files, jps) are described in the GNSS Receiver External Interface Specification available on the official website of the company www.javad.com [GREIS, 2010]. This allows us to create our own receiver software and gain additional information, which is usually lost when internal receiver files are converted to RINEX format (amplitude, signal quadrature, etc.). In order to provide automatic operation of SibNet receivers under the operating system (OS) Linux, ISTP SB RAS has developed software designed to control and collect data from the Javad Delta-G3T dual-frequency GNSS receiver via USB and RS-232 interfaces in Linux [Perevalov, Perevalova, 2016].

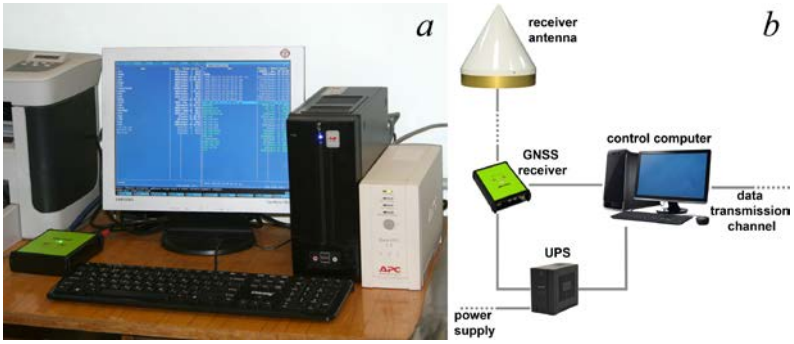

Figure 2. Appearance (*a*) and layout (*b*) of equipment of the GNSS measuring array installed at observation stations

Figure 3. Stages of installation of a GNSS antenna on a bedrock base at the observation station UZUR (*a*–*b*)

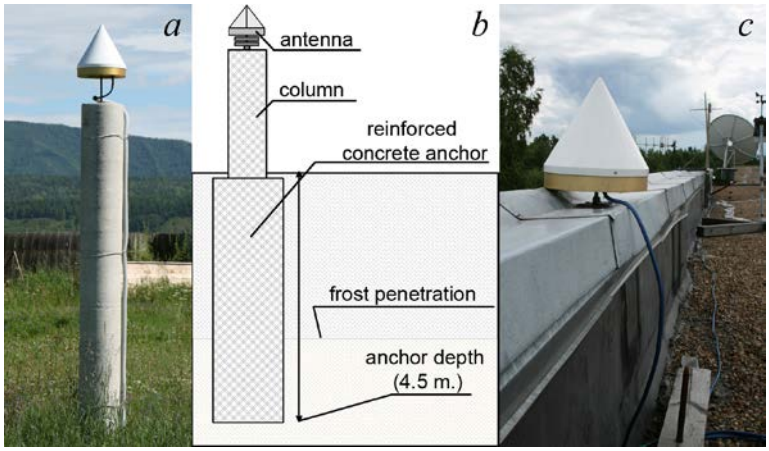

Figure 4. Appearance of a reinforced concrete base (*a*) and scheme of its mounting on sedimentary/mantle rocks at TORY (*b*); an antenna on the roof of the established permanent structure ORDA (*c*)

Table 2

Characteristics of SibNet stations in the Baikal region

Station	Station type	Receiver type	Base type for antenna	Starting date of regular observations
TORY	Constant	SigmaQ-G3D	Reinforced concrete anchor	March 20, 2012
LIST	Constant	Delta-G3T	Solid rock	June 15, 2012
ORDA	Constant	Delta-G3T	Permanent structure	June 14, .2011
UZUR	Constant	Delta-G3T	Solid rock	March 21, 2013
MOND	Constant	Delta-G3T	Solid rock	September 11, 2013
ISTP	Constant	Delta-G3T	Permanent structure	April 01, 2012
SARM	Constant	Delta-G3T	Roof of a wooden building	December 02, 2012
MKSM	Temporary	Delta-G3T	Roof of a wooden building	April 27, 2014
ZAKT	Temporary	Delta-G3T	Wooden post	irregular
ZMUR	Temporary	Delta-G3T	Wooden post	irregular
BDRY	Temporary	Delta-G3T	Roof of a permanent structure	irregular
PATR	Temporary	Delta-G3T	Roof of a wooden building	irregular
BBSH	Temporary	Delta-G3T	Roof of a wooden building	irregular
SHCH	Temporary	Delta-G3T	Roof of a wooden building	irregular

The software is implemented as a console-based application of OS Linux and can be executed both in interactive and batch modes. It allows us to specify measurement parameters, obtain measurement data at a given sampling rate, monitor the integrity of the data, correct consequences of technical failures in the data, file the data to hard disk in JPS format (standard format of JAVAD GNSS receiver files [GREIS, 2010]).

The receivers used in SibNet do not have a built-in memory for recording measurements; therefore they are connected to the control computer (Figure 2) for temporary storage and subsequent transfer of data to the data center located at ISTP SB RAS. In the standard mode, SibNet receivers record signal parameters at a frequency of 1 Hz. For individual experiments, we employ modes with increasing recording frequency up to 50 Hz.

GNSS RADIO PATHS COVERING THE SOUTHERN BAIKAL REGION

Each GNSS receiver at any time receives signals from at least 8 GPS satellites and 7 GLONASS satellites. In ionospheric research, the visible movement of GNSS satellites is generally represented by the movement of ionospheric points. An ionospheric point is the place where the receiver–GNSS satellite radio path intersects with a conditional thin sphere located at a height h_{max} of the main maximum of electron density in the ionosphere. This height has been chosen because the region located near the main ionization maximum makes the maximum contribution to TEC. In general, this height has seasonal, diurnal, and other dependencies and can vary from 200 to 400 km. For each satellite, the ionospheric point can be remote from a receiver at 15° in longitude and latitude (Figure 5).

The rotation period of GPS satellites (11 hrs 58 min) is selected in such a way that every day a satellite flies along the same trajectory relative to a stationary terrestrial observer. The rotation period of GLONASS satellites (11 hrs 15 min) is selected in such a way that the position of the GLONASS satellite trajectory shifts by 22.5° relative to Earth per day, i.e. the satellite repeats its trajectory relative to a terrestrial observer in 8 days.

Movement of GNSS satellites around the sky, on the one hand, causes certain difficulties: 1) TEC variations have a trend associated with unequal effective thickness of the ionosphere at different elevation angles of satellites (Figure 6, *a*); 2) there is an additional difficulty in determining velocities and directions of traveling ionospheric disturbances.

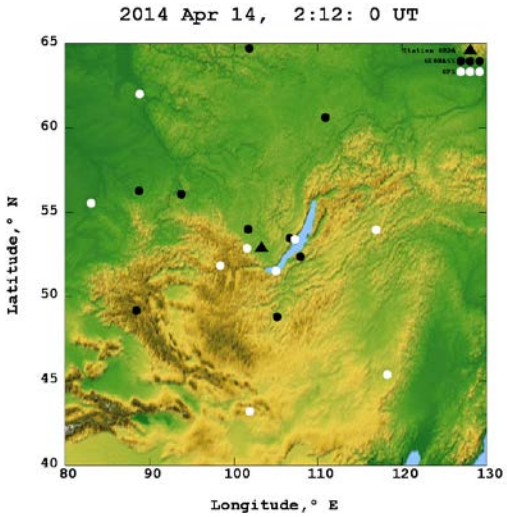

Figure 5. Position of ionospheric points of GLONASS (black dots) and GPS (white dots) satellites for the ORDA receiver (triangle) at a given time

On the other hand, the movement of GNSS satellites makes it possible to scan the entire sky per calendar day with one receiver. For example, Figure 7 shows positions of ionospheric points for GLONASS and GPS satellites, obtained per calendar day from MOND data. Thus, one mid-latitude station can scan an ionospheric region of about 30° in latitude and more than 40° in longitude.

Figure 7 indicates that there is a certain "blind" zone in a northerly direction, i.e. a part of the sky without GNSS satellites. This is due to the inclination of orbits of GNSS satellites. For GPS, orbit inclination to the equator is on the average 55°; for GLONASS, 64.8°

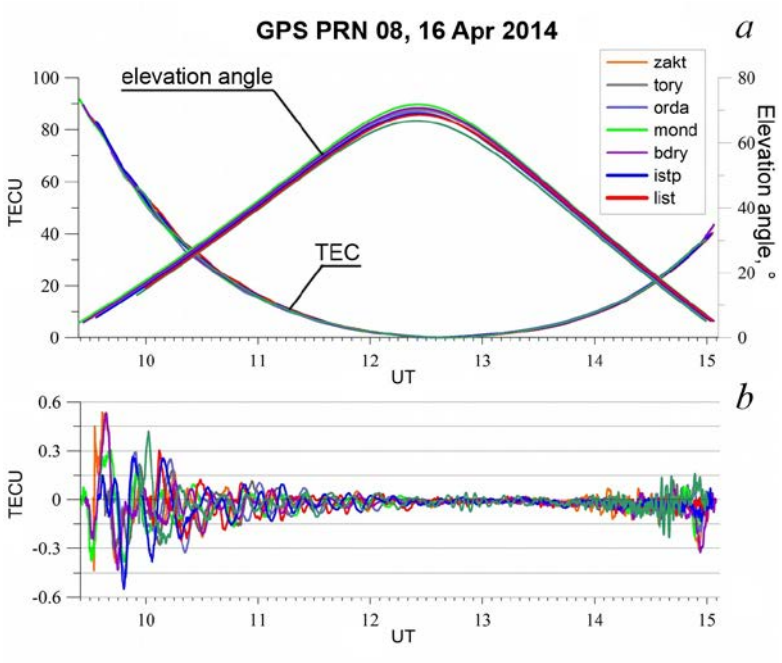

Figure 6. TEC variations obtained from signals of one satellite at spaced stations: unfiltered variations with a temporal trend associated with the satellite's elevation angle (*a*); the same variations filtered by a moving average with a 0.5–10 min time window (*b*)

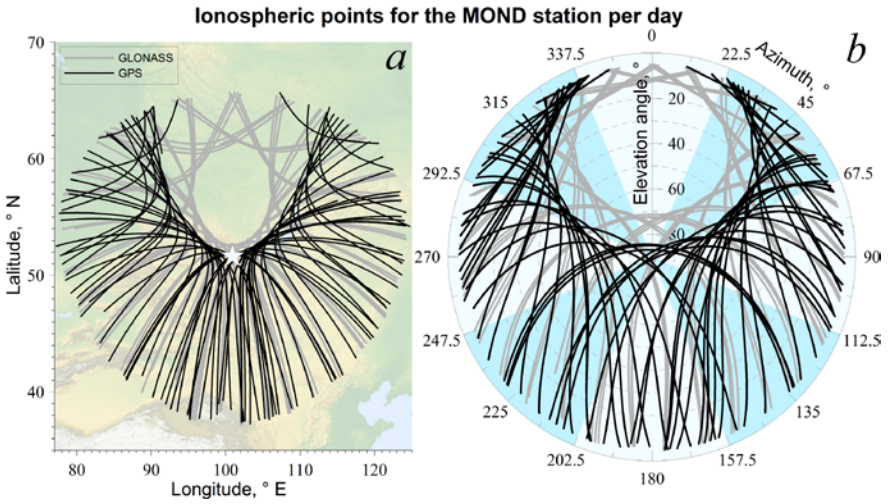

Figure 7. Ionospheric points for the MOND station per day in coordinates longitude–latitude (*a*) and elevation angle–azimuth of a GNSS satellite (*b*) for all available satellites. Gray lines show ionospheric points for GLONASS; black, for GPS

(the real orbit inclinations can significantly differ from calculated ones, for example, for the GPS system they vary from 51 to 57°). Figure 7 shows that the blind zone for GLONASS is much smaller. Therefore, in terms of territory coverage for ionospheric research in middle and high latitudes, GLONASS is more preferable than GPS.

FIRST RESULTS OF RECORDING OF IONOSPHERIC EFFECTS INDUCED BY PROGRESS CS ENGINE

SibNet along with other ISTP SB RAS instruments has been used to record ionospheric effects of operation of Progress CS engine. To make the network of GNSS stations denser, we deployed temporary receiving stations (Figure 1). Since long-term data series from these stations are not used for geodynamic measurements, requirements for installation of antennas are not so strict as for permanent stations. In particular, for ionospheric measurements during active SE in 2014–2016, temporary antennas were mounted on wooden posts, roofs of buildings, etc. (Figure 8).

We calculate TEC variations from GLONASS/GPS data with a single standard technique based on GNSS dual-frequency phase measurements [Hofmann-Wellenhof et al., 1992]. In high-accuracy GNSS phase measurements, the error in determining TEC does not exceed 0.01 TECU [Hofmann-Wellenhof et al., 1992]. This allows us to detect sufficiently weak disturbances. We calculate TEC from

both GPS and GLONASS data. Initial series of TEC variations (Figure 6, *a*) are filtered by the moving average method [Afraimovich, Perevalova, 2006] in a range 0.5–10 min (Figure 6, *b*). Since it is known that the height of Progress CS flight was about 400 km [Khakhinov et al., 2011, 2012; Hakhinov et al., 2012, 2013], we calculate coordinates of ionospheric points for this height (h_{max}=400 km).

During the experiments on detection of ionospheric effects of active influence of Progress CS jet stream, we employed a method of mapping ionospheric disturbances [Perevalova et al., 2008; Tsugawa et al., 2011; Kunitsyn et al., 2011; Perevalova et al., 2012; Afraimovich et al., 2013; Astafyeva et al., 2013]. The method means that for each current moment the position of ionospheric points is plotted on a map for all receiver—satellite rays, and the color of points corresponds to the current value of TEC variation amplitude in this ray, which is an indicator of ionospheric disturbances. The method allows us to visually trace the spatio-temporal dynamics of TEC disturbances. When studying TIDs, constructing a sequence of such maps for adjacent time points is a very convenient tool for visual evaluation of TID parameters such as intensity, velocity, and direction.

Position of ionospheric points on the map gives a graphic representation of the geometry of the April 16, 2014 experiment (Figure 9). It can be seen that there are both negative and positive TEC disturbances. The local nature of the effect of operation of CS engines on the ionosphere required a careful analysis of data obtained in radio paths passing near the disturbed region and crossing it. To conduct this analysis, we mapped the disturbed region by plotting ionospheric points for the PRN 08 GPS satellite (Figure 10).

The ionospheric points for this satellite and different stations crossed the disturbed region in 9 min (Figure 10, *a*) and 22 min (Figure 10, *b*). Figure 11 shows TEC variations for this satellite at different GNSS stations. The moment when the ionospheric point of the PRN08–LIST ray intersects the disturbed region (Figure 10, *b*) corresponds to the moment of the maximum decrease in TEC in LIST data for the PRN 08 GPS satellite (Figure 11, the moment is indicated by a vertical red line). This fact suggests a connection between the active effect and the observed minimum, despite that in data from other stations there are TEC variations with comparable intensities. The amplitude of the observed disturbance is 0.07 TECU, which exceeds the error in determining TEC (0.01 TECU) and the level of background variations at close elevation angles of the satellite (~0.02 TECU). On April 16, 2014, there were no strong geomagnetic disturbances: the K_p index did not exceed 1.3 for the last 6 hrs before the experiment. Taking into account the spatio-temporal localization of the TEC minimum and the locality of the effect, we can conclude that it is the effect of the jet stream that causes a decrease in electron density.

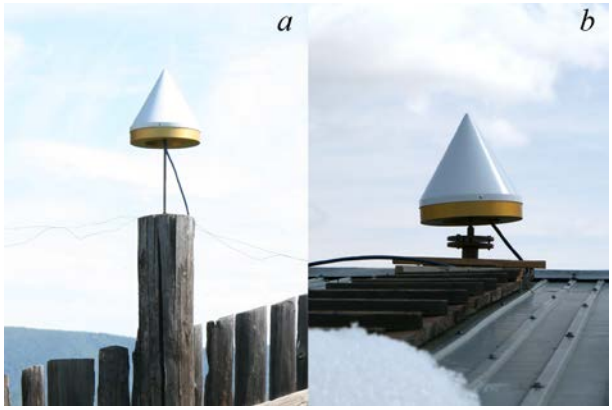

Figure 8. Antennas of temporary observation stations mounted on a wooden fence post (*a*) and on the roof of a building (*b*)

However, such decreases in TEC variations are not always observed. When another ionospheric point (PRN08–ISTP radio path) crosses the disturbed region (Figure 11), there is no significant decrease in TEC in this path. This seems to be associated with the long interval between the engine start and the passage of the ionospheric point through the disturbed region (Figure 11, vertical blue line).

The above cases when the ionospheric points intersected the disturbed area occurred under a very favorable geometry of measurements: the elevation angle of the PRN 08 GPS satellite was maximum for the current data series (Figure 6, *a*).

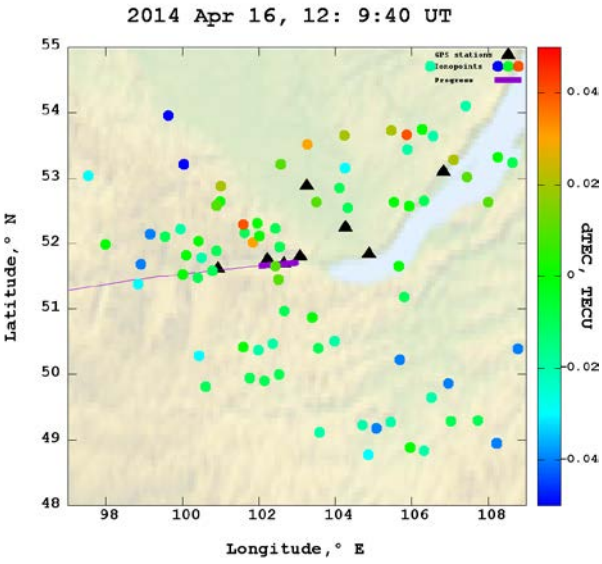

Figure 9. Ionospheric points for SibNet during the April 16, 2014 experiment. The color of the point shows the instantaneous value of TEC variations in the corresponding satellite–receiver ray. Triangles mark GNSS stations; the solid line is the trajectory of Progress cargo spacecraft; the thickened section of the trajectory indicates the Progress CS with operating engine

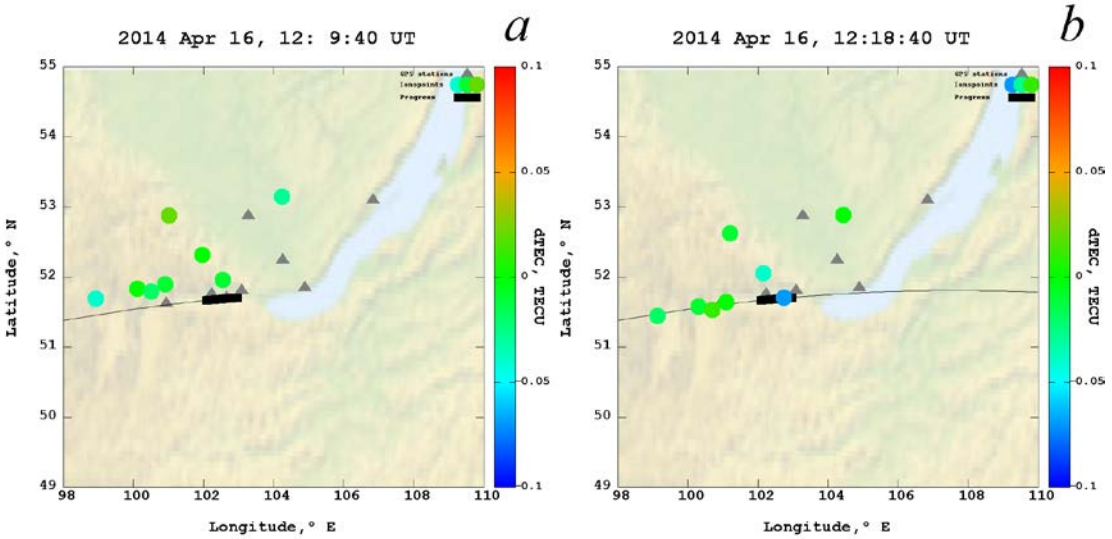

Figure 10. Ionospheric points for the PRN 08 GPS satellite during the April 16, 2014 experiment. Notations are the same as in Figure 9

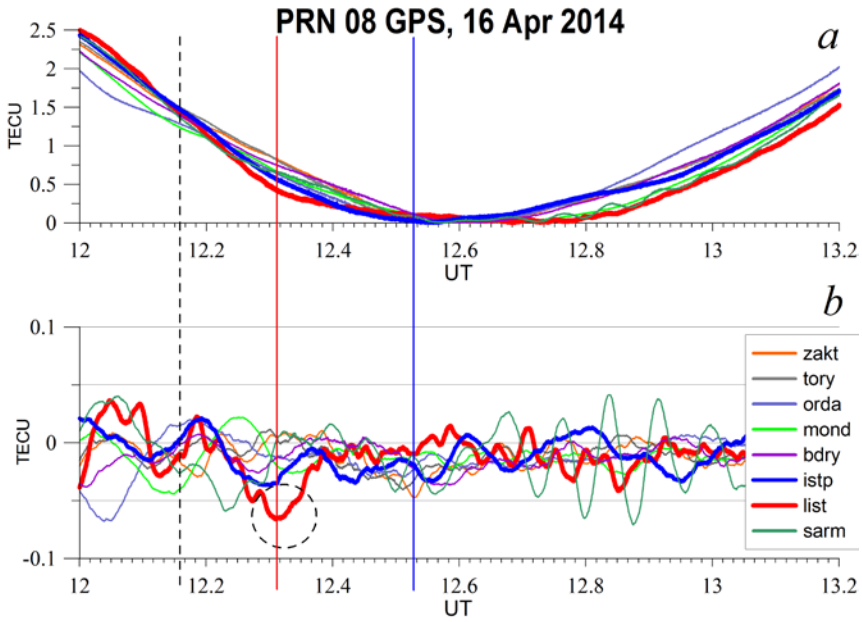

Figure 11. Data on TEC variations obtained from signals of the PRN 08 GPS satellites at spaced stations: unfiltered data (*a*); the same data filtered by a moving average with a 2–10 min time window (*b*). The vertical dashed line indicates the moment of engine start

This allowed us to avoid recording of high-amplitude TEC variations, which occurred two hours before and two hours after the engine start (Figure 6, *a*). This geometry of the experiment was extremely successful for detecting the response to the Progress cargo spacecraft engine impact.

A detailed analysis of parameters of the ionospheric response to the effect of CS engines in all active experiments is carried out in [Ishin et al., 2017].

CONCLUSION

The deployment of the network of dual-frequency GNSS receivers (SibNet) in the Southern Baikal region provides an effective instrument for monitoring ionospheric conditions. Antennas being mounted on specially equipped bases, data from this network can additionally be used to study the movement of lithospheric plates, which is also a topical problem for the seismically active Baikal rift system.

SibNet operates in a continuous mode, thus allowing us not only to conduct pre-planned experiments, but also to study geophysical responses to complex unpredictable phenomena such as earthquakes, meteoric impacts, explosions of fireballs in the atmosphere, etc.

The method of mapping ionospheric disturbances, which has been repeatedly used for detecting TIDs [Perevalova et al., 2008; Tsugawa et al., 2011; Kunitsyn et al., 2011; Perevalova et al., 2012; Afraimovich et al., 2013; Astafyeva et al., 2013; Yasyukevich et al., 2015; Zakharov et al., 2016], has demonstrated its effectiveness in detection of local disturbances. We have identified relatively weak and vertically localized disturb-

ances caused by the effect of the Progress spacecraft engine in the April 16, 2014 experiment. Using this method, we have shown that these disturbances can be unambiguously associated with the Progress CS engine impact.

Thus, the deployment of SibNet has greatly expanded the possibilities of studying local geophysical events, and also has supplemented the worldwide network of GNSS stations. The first results, obtained via SibNet, prove the effectiveness of the use of such networks, in particular during active experiments in Earth's ionosphere.

The work was carried out under the project No. AAAA-A16-116012210460-0 "Investigation of the lithosphere–atmosphere–ionosphere system under extreme conditions" of RAS Presidium Program No.15 with the support of RFBR grant No. 16-35-00027_mol_a "Studying ionospheric response to simultaneous influence of various sources in the neutral atmosphere" 2016–2017. Experimental data were obtained with the Angara Multiaccess Center facilities at ISTP SB RAS.

REFERENCES

Afraimovich E.L. GPS global detection of the ionospheric response to solar flares. *Radio Sci.* 2000, vol. 35, no. 6, pp. 1417–1424.

Afraimovich E.L., Astafyeva E.I., Demyanov V.V., Edemsky I.K., Gavrilyuk N.S., Ishin A.B., Kosogorov E.A., Leonovich L.A., Lesyuta O.S., Palamarchuk K.S., Pere-valova N.P., Polyakova A.S., Smolkov G.Ya., Voeykov S.V., Yasyukevich Yu.V., Zhivetiev I.V. A review of GPS/GLONASS studies of the ionospheric response to natural and anthropogenic processes and phenomena. *J. Space Weather Space Climate.* 2013, no. 3, pp. A27_p1–A27_p19. DOI: 10.1051/swsc/2013049.

Afraimovich E.L., Perevalova N.P. *GPS-monitoring verhnei atmosfery Zemli* [GPS-monitoring of the Earth's upper atmosphere]. Irkutsk, 2006, 480 p. (In Russian).

Afraimovich E.L., Voeykov S.V., Perevalova N.P., Vodyannikov V.V., Gordienko G.I., Litvinov Yu.G., Yakovets A.F. Ionospheric effects of the March 29, 2006, solar eclipse over Kazakhstan. *Geomagnetism and Aeronomy*. 2007, vol. 47, no. 4, pp. 461–469.

Astafyeva E., Rolland L., Lognonne P., Khelfi K., Yahagi T. Parameters of seismic source as deduced from 1 Hz ionospheric GPS data: Case study of the 2011 Tohoku-Oki event. *J. Geophys. Res. Space Phys.* 2013, vol. 118, pp. 5942–5950. DOI: 10.1002/jgra.50556.

Beletsky A.B., Mikhalev A.V., Khakhinov V.V., Lebedev V.P. Optical manifestation of functioning onboard engines of low-orbit spacecraft. *Solar-Terr. Phys.* 2016, vol. 2, no. 4, pp. 85–91.

Borisov B.S., Gabdullin F.F., Garkusha V.I., Korsun A.G., Kurshakov M.Yu., Strashinsky V.A., Tverdokhlebova E.M., Khakhinov V.V. Radiophysical characteristics of low-orbit spacecraft plasma environment revealed by space experiments. *Nelineinyi mir* [J. Nonlinear World]. 2012, vol. 10, no. 10, pp. 700–709. (In Russian).

Demyanov V.V., Afraimovich E.L., Jin S. An evaluation of potential solar radio emission power threat on GPS and GLONASS performance. *GPS Solutions*. 2012, vol. 16, no. 4, pp. 411–424.

Demyanov V.V., Yasyukevich Yu.V. Deterioration in the accuracy of GPS system positioning due to the effect of ionospheric bubbles. *Geomagnetism and Aeronomy*. 2011, vol. 51, no. 7, pp. 1010–1013.

Ding F., Wan W., Mao T., Wang M., Ning B., Zhao B., Xiong B. Ionospheric response to the shock and acoustic waves excited by the launch of the Shenzhou-10 spacecraft. Geophys. Res. Let., 2014, vol. 41, pp. 3351–3358.

Eselevich M.V., Khakhinov V.V., Klunko E.V. Parameters of optical signals registered with the AZT-33IK telescope in active radar-progress space experiment. *Solar-Terr. Phys.* 2016, vol. 2, no. 3, pp. 32–43.

GREIS: GNSS Receiver External Interface Specification. Version 3.2.0. Javad GNSS. 2010. Available at: www.javad.com/jgnss/support/manuals.html (accessed 12 May 2017).

Hofmann-Wellenhof B., Lichtenegger H., Collins J. *Global Positioning System: Theory and Practice*. New York. Springer-Verlag Wien, 1992, p. 327.

Institut solnechno-zemnoi fiziki: sozdanie i razvitie. Ed. Zherebtsov G.A. [Institute of Solar-Terrestrial Physics: Foundation and Development. Ed. Zherebtsov G.A.]. Novosibirsk: SB RAS Publ., 2015, 610 p.

Ishin A.B., Perevalova N.P., Voeykov S.V., Khakhinov V.V. Complex analysis of the ionospheric response to operation of Progress cargo spacecraft according to the data of GNSS receivers in Baikal region. Solar-Terr. Phys. 2017, vol. 3, no. 4, pp. 93–103. (In Russian).

Jiao Y., Morton Y.T., Taylor S., Pelgrum W. Characterization of high-latitude ionospheric scintillation of GPS signals, *Radio Sci*. 2013, vol. 48, iss. 6, pp. 698–708.

Khakhinov V.V., Potekhin A.P., Lebedev V.P., Alsatkin S.S., Ratovsky K.G, Kushnarev D.S., Tverdokhlebova E.M., Kurshakov M.Yu., Manzheley A.I., Timofeeva N.I. Results of remote sounding of ionospheric disturbances during active experiments Radar–Progress. *Sovremennye problemy distantsionnogo zondirovaniya Zemli iz kosmosa* [Current problems in remote sensing of Earth from space]. 2012, vol. 9, no. 3, pp. 199–206. (In Russian).

Khakhinov V.V., Potekhin A.P., Lebedev V.P., Medvedev A.V., Kushnarev D.S., Shpynev B.G., Zarudnev V.E., Alsatkin S.S., Ratovsky K.G, Podlesny A.V., Bryn'ko I.G. Radio physical methods of diagnostics of the ionospheric disturbances generated by onboard engines of TCS Progress: algorithms, tools and results. *Zhurnal radioelektroniki. Rossiiskaya nauchnaya konferentsiya "Zondirovanie zemnykh pokrovov radarami s sintezirovannoi aperturoi"*. Ulan-Ude, 06.09–10.09.2010. [J. Radio Electronics. Proc. the Russian Scientific Conference "Sounding of Terrestrial Covers Using Radars with the Synthesized Aperture. Ulan-Ude, 06.09–10.09.2010]. 2010, p. 553–569. (In Russian).

Khakhinov V., Potekhin A., Shpynev B., Alsatkin S., Ratovsky K., Lebedev V., Kushnarev D. Results of complex radio sounding of ionospheric disturbances generated by the transport spacecraft Progress onboard thrusters. Proc. 30th URSI General Assembly and Scientific Symposium. 2011. Available at: http://www.ursi.org/proceedings/procGA11/ursi/HP2-15.pdf (accessed 12 May 2017).

Khakhinov V.V., Potekhin A.P., Lebedev V.P., Kushnarev D.S., Alsatkin S.S. Some results of Plasma–Progress and Radar–Progress active space experiments. *Vestnik Sibirskogo gosudarstvennogo aerokosmicheskogo universiteta im. akademika M.F. Reshetneva* [Bull. M.F. Reshetnev Siberian State Space University]. 2013, special iss., vol. 5, no. 51, pp. 160–162. (In Russian).

Khakhinov V.V., Shpynev B.G., Lebedev V.P., Kushnarev D.S., Alsatkin S.S., Khabituev D.S. Radio sounding of ionospheric disturbances generated by exhaust streams of the transport spacecraft Progress engines. Proc. PIERS-2012. Moscow, 2012, pp. 1168–1171.

Klunko E.V., Eselevich M.V., Tergoev V.I. Progress cargo spacecraft observed with the AZT-33IK optical telescope. *Solar-Terr. Phys.* 2016, vol. 2, no. 3, pp. 22–31.

Kunitsyn V.E., Nesterov I.A., Shalimov S.L. Japan mega-thrust earthquake on March 11, 2011: GPS-TEC evidence for ionospheric disturbances. *J. Experimental and Theoretical Phys. Lett.* (JETP Lett.). 2011, vol. 94, no. 8, pp. 616–620.

Lebedev V.P., Khakhinov V.V., Kushnarev D.S., Podlesny A.V., Garkusha V.I. Radiophysical effects of spacecraft engine burn. *Trudy XXIV vserossiiskoi konferentsii po rasprostraneniju radiovoln* [Proc. 24th National Conference "Propagation of Radio Waves". Irkutsk. June 29 – July 5 2014]. 2014, vol. 1, pp. 60–66. (In Russian).

Lejeune S, Wautelet G, Warnant R Ionospheric effects on relative positioning within a dense GPS network. *GPS Solutions*. 2012, vol. 16, no. 1, pp. 105–116.

Lipko Yu.V., Pashinin A.Yu., Rakhmatulin R.A., Khakhinov V.V. Geomagnetic effects caused by rocket exhaust jets. *Solar-Terr. Phys.* 2016, vol. 2, no. 3, pp. 43–55.

Liu J.Y., Lin C.H. Ionospheric solar flare effects monitored by the ground based GPS receivers: theory and observation . *J. Geophys. Res.* 2004, vol. 109, A01307.

Perevalov A.A., Perevalova N.P. The control and data acquisition with dual-frequency GNSS receiver Javad Delta vi interfaces USB and RS-232 in interactive and batch modes i the Linux operating system. *Certificate of State Registration o Program for Computer № 2016613942. 12.04.2016.* (In Russian).

Perevalova N.P., Afraimovich E.L., Voeykov S.V., Zhivetiev I.V. TEC disturbances during strong magnetic storm on October 29, 2003. *J. Geophys. Res.* 2008, vol. 113, A00A13. DOI: 10.1029/2008JA013137.

Perevalova N.P., Voeykov S.V., Yasyukevich Yu.V., Ishin A.B., Voeykova E.S., Sankov V.A. Investigation into ionospheric disturbances caused by the earthquake of 11 March 2011 in Japan, using GEONET data. *Sovremennye problemy distantsionnogo zondirovaniya Zemli iz kosmosa* [Current problems in remote sensing of Earth from space]. 2012, vol. 9, no. 3, pp. 172–180. (In Russian).

Prikryl P., Jayachandran P.T., Mushini S.C., Pokhotelov D., MacDougall J.W., Donovan E., Spanswick E., St.-Maurice J.-P. GPS TEC, scintillation and cycle slips observed at high latitudes during solar minimum. *Ann. Geophys*. 2010, vol. 28, pp. 1307–1316.

Seismoionosfernye i seismoelektromagnitnye protsessy v Bajkal'skoi riftovoi zone. Ed. Zherebtsov G.A. [Seismoionospheric and Seismoelectromagnetic Processes in the Baikal Rift Zone. Ed. Zherebzov G.A.]. Novosibirsk, SB RAS Publ., 2012. 304 p. (In Russian).

Shimeis A., Borries C., Amory-Mazaudier C., Fleury R., Mahrous A.M., Hassan A.F., Nawar S. TEC variations along an East Euro-African chain during 5th April 2010 geomagnetic storm. *Adv. Space Res*. 2015, no. 55, pp. 2239–2247.

Shpynev B.G., Alsatkin S.S., Khakhinov V.V., Lebedev V.P. Investigating the ionosphere response to exhaust products of Progress cargo spacecraft engines on the basis of Irkutsk incoherent scatter radar data. *Solar-Terr. Phys*. 2017, vol. 3, no. 1, pp. 114–127.

Spogli L., Alfonsi L., Cilliers P.J., Correia E., Franceschi G., Mitchell C.N., Romano V., Kinrade J., Cabrera M. A. GPS scintillations and total electron content climatology in the southern low, middle and high latitude regions. *Annals of Geophys.* 2013, vol. 56, no. 2, R0220.

Tsugawa T., Saito A., Otsuka Y., Nishioka M., Maruyama T., Kato H., Nagatsuma T., Murata K.T. Ionospheric disturbances detected by GPS total electron content observation after the 2011 Tohoku Earthquake. *Earth, Planets and Space*. 2011, vol. 63, no. 7, pp. 875–879.

Yasyukevich Y.V., Voeikov S.V., Zakharov V.I., Kunitsyn V.E. The response of the ionosphere to the earthquake in Japan on March 11, 2011 as estimated by different GPS-based methods. *Geomagnetism and Aeronomy*. 2015, vol. 55, no 1, pp. 108–117.

Zakharov V.I., Yasyukevich Y.V., Titova M.A. Effect of magnetic storms and substorms on GPS slips at high latitudes. *Cosmic Res.* 2016, vol. 54, no 1, pp. 20–30.

Zherebtsov G.A., Perevalova N.P. Ionospheric response to a rocket launch from the Vostochnyi Cosmodrome. *Doklady akademii nauk. Nauki o Zemle* [Doklady Earth Sciences]. 2016, vol. 471, part 2, pp. 1280–1283.

How to cite this article

Ishin A.B., Perevalova N.P., Voeykov S.V., Khakhinov V.V. First results of registering ionospheric disturbances obtained with the SibNet network of GNSS receivers in active space experiments. *Solar-Terrestrial Physics.* 2017. Vol. 3, No. 4, P. 74–82. DOI: 10.12737/stp-34201708